Astronomy & Astrophysics manuscript no. aa55315-25
July 18, 2025
©ESO 2025

Letter to the Editor

More than 60% of double-peaked narrow emission lines not related to dual galaxy systems?

XueGuang Zhang

Guangxi Key Laboratory for Relativistic Astrophysics, School of Physical Science and Technology, GuangXi University, No. 100, Daxue Road, Nanning, 530004, P. R. China e-mail: xgzhang@gxu.edu.cn

July 18, 2025

arXiv:2507.12893v1 [astro-ph.GA] 17 Jul 2025

ABSTRACT

Dual galaxy system (DGS) is one of the widely accepted scenarios to explain the double-peaked narrow emission lines (DPNELs) due to orbital motions of the two galaxy in a merging system. After considering no physical connections between two independent narrow emission line regions in two galaxies in one DGS, there should be no correlations between flux ratios R_R of red-shifted narrow emission components from one galaxy and flux ratios R_B of blue-shifted narrow emission components from the other galaxy in the DGS. However, after checking the large sample of DPNELs in the SDSS, there are strong linear correlations in different groups between R_R as the flux ratio of red-shifted narrow [O III] to the red-shifted narrow Hα and R_B as the flux ratio of blue-shifted narrow [O III] to the blue-shifted narrow Hα. Meanwhile, after checking narrow emission line properties of galaxy pairs within 30 (20, 10) arcmins, there are no connections between narrow emission line fluxes in the galaxy pairs, to support the detected linear correlations being robust enough between R_R and R_B in the DPNELs in SDSS. Furthermore, through oversimplified simulations, at least more than 60% of the DPNELs should be not related to the expected DGSs.

Key words. galaxies:active - galaxies:nuclei - quasars: supermassive black holes - quasars:emission lines

1. Introduction

Narrow emission lines from central narrow emission line regions (NLRs) are fundamental optical spectroscopic characteristics of emission line galaxies, such as active galactic nuclei (AGN) and HII galaxies. Moreover, among emission line galaxies, there is one unique subclass, the emission line galaxies with double-peaked narrow emission lines (DPN galaxies). Since the first DPN galaxy reported in Zhou et al. (2004), more 10000 DPN galaxies have been reported, such as the samples in Comerford et al. (2009); Wang et al. (2009); Smith et al. (2010); Ge et al. (2012); Wang et al. (2019); Ge et al. (2020); Zheng et al. (2025).

In order to explain the double-peaked narrow emission lines (DPNELs), the following two main scenarios have been proposed. First, two independent NLRs related to two galaxies merging as a dual galaxy system (DGS) can normally lead to DPNELs due to orbital motions of the two galaxies, as natural products of hierarchical galaxy formation and evolution (Silk & Rees 1998; Cole et al. 2000; Volonteri et al. 2003; Merritt 2006; De Lucia & Blaizot 2007; Satyapal et al. 2014; Zoldan et al. 2019; Yoon et al. 2022; Attard et al. 2024). Second, local dynamic structures (such as radial flows, rotating disks) in NLRs in individual galaxy can also lead to DPNELs, such as the discussions in Shen et al. (2011); Fu et al. (2012); Nevin et al. (2006); Comerford et al. (2018); Rubinur et al. (2019).

It is clear that not all the DPN galaxies can be accepted as indicators of DGSs, but it is not clear that the proportion of DPN galaxies are not related to DGSs. Here, an independent method is proposed to determine the proportion of DPN galaxies not related to DGSs. Assumed DPNELs related to DGSs, corresponding spatial separation of the two galaxy in one DGS should be longer enough that narrow line emission properties were self-governed by each individual galaxy in the DGS, otherwise more complicated profiles should be expected rather than apparent double-peaked features. In other words, very weak intrinsic connections could be expected between narrow emission lines from the two galaxies in one DGS leading to DPNELs. Therefore, to check emission property connections between the red-shifted components and the blue-shifted components in DPNELs will provide meaningful clues to support or to be against the DPNELs related to the proposed DGSs, which is our main objective.

The manuscript is organized as follows. Section 2 presents the main results and necessary discussions on tight flux correlations between the red-shifted components and the blue-shifted components in DPNELs. The main summary and conclusions are given in Section 3. In the manuscript, we have adopted the cosmological parameters of H_0=70 km s^{-1} Mpc^{-1}, Ω_m=0.3, and Ω_Λ=0.7.

2. Main results and necessary discussions

The DPN galaxies, collected from the public sample reported in Ge et al. (2012), have been classified into five groups through properties of narrow/broad emission lines. In Ge et al. (2012), through the spectra of main galaxies in SDSS DR7, after removing the host galaxy contributions determined by the STARLIGHT, the emission lines are measured by multiple Gaussian functions. After checking the best-fitting results to the emission lines by the F-test technique, about 3030 DPN galaxies have been collected with apparent DPNELs with significance levels higher than 3σ. Moreover, we do not consider the more than 10000 galaxies collected with asymmetric or top-flat profiles of emission lines in Ge et al. (2012). Meanwhile, in order to check

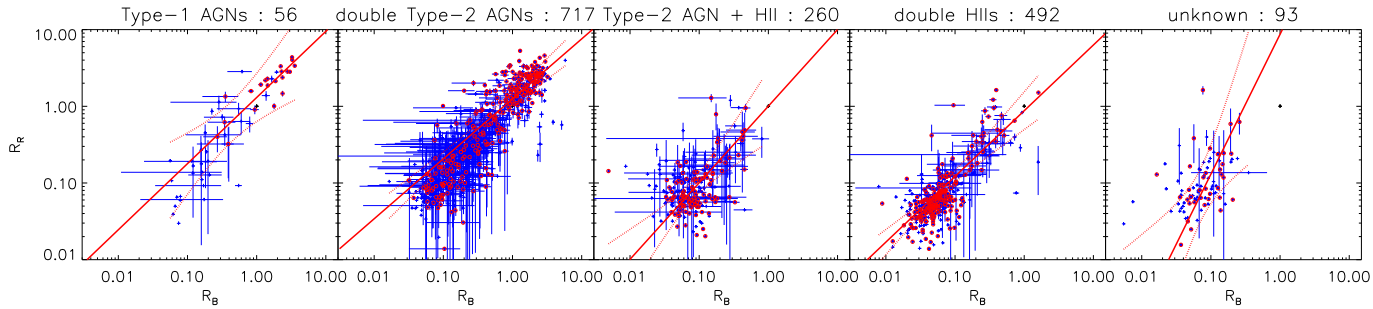

Fig. 1. On the correlations between R_R and R_B for the SDSS objects with apparent DPNELs in the five groups. In each panel, solid red line and dashed red lines show the best fitting results and the corresponding 3σ confidence bands. In each panel, open red circles mark the galaxies with larger R_{ps}.

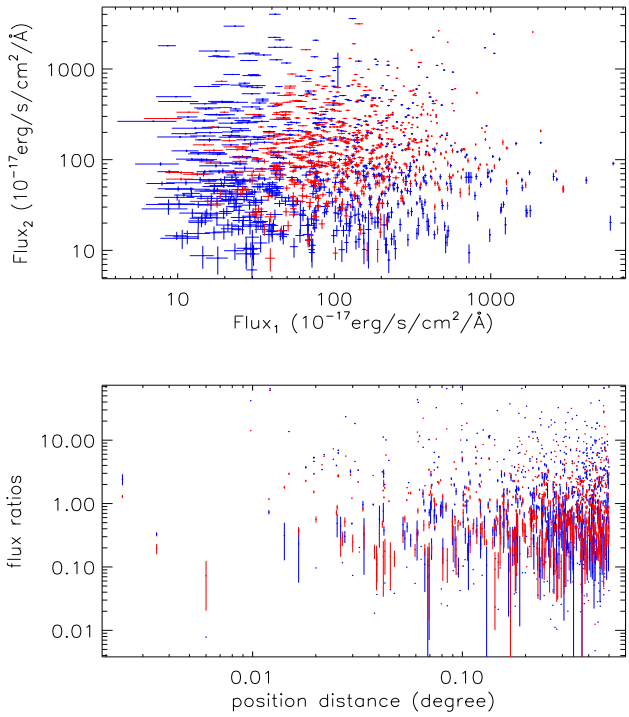

Fig. 2. Top panel shows the flux correlations of narrow emission lines of both [O III]λ5007Å (in blue) and narrow Hα (in red) in the 669 AGN pairs with redshift difference smaller than 0.001 and with position distance smaller than 30 arcmins. Bottom panel shows the dependencies of narrow emission line flux ratios on position distance. In bottom panel, symbols in blue and in red show the flux ratios of [O III]λ5007Å and the flux ratios of narrow Hα in the 669 AGN pairs, respectively.

the probable correlation between R_B (flux rations of the blue-shifted components in DPNELs) and R_R (flux rations of the red-shifted components in DPNELs), the 1618 of 3030 galaxies are collected from Ge et al. (2012) with the measured line fluxes of the blue/red-shifted emission components in [O III] and in narrow Hα at least five times larger than their corresponding uncertainties. Among the 1618 galaxies, considering the appearance of broad Hα, the first group (G1) includes 56 Type-1 AGNs. For the other 1562 galaxies, assumed the DGSs for the DPNELs, the measured emission fluxes of the blue-shifted and the red-shifted components in the DPNELs can be applied to determine the classifications of the two individual galaxies in the assumed DGS, through the commonly applied BPT diagrams (Baldwin et al. 1981; Kewley et al. 2001; Kauffmann et al. 2003; Kewley et al. 2006, 2019; Zhang et al. 2020). Then, the second group (G2) includes 717 galaxies with each individual galaxy classified as Type-2 AGN. The third group (G3) includes 260 galaxies with one individual galaxy classified as Type-2 AGN but the other individual galaxy classified as HII galaxy. The four group (G4) includes 492 galaxies with each individual galaxy classified as HII galaxy. The fifth group (G5) includes 93 galaxies with one individual galaxy not classified by BPT diagrams due to lack of emission components of some narrow emission lines.

Through the reported emission line fluxes of the red-shifted and blue-shifted components in both narrow [O III] and narrow Hα for the 1618 galaxies included in the five groups, Fig. 1 shows the correlations between R_B (flux ratio of the blue-shifted component in [O III] to the blue-shifted component in narrow Hα) and R_R (flux ratio of the red-shifted component in [O III] to the red-shifted component in narrow Hα). For all the 1618 galaxies, the Spearman Rank correlation coefficient is about 0.65 ($P_{null} < 10^{-21}$). Meanwhile, for the galaxies in G1, G2, G3, G4, G5 groups, corresponding Spearman Rank correlation coefficients are about 0.90 ($P_{null} \sim 1.2 \times 10^{-21}$), 0.88 ($P_{null} < 10^{-21}$), 0.31 ($P_{null} \sim 6 \times 10^{-7}$), 0.63 ($P_{null} < 10^{-21}$), 0.48 ($P_{null} \sim 1.5 \times 10^{-6}$), respectively.

Furthermore, considering the uncertainties in both coordinates, through the Least Trimmed Squares regression technique (Cappellari et al. 2013; Mahdi & Mohammad 2017), the linear correlations shown in Fig. 1 can be described as

$$\begin{aligned}
\log(R_R) &= 0.10 \pm 0.01 + (0.82 \pm 0.02)\log(R_B) \quad (ALL)\\
\log(R_R) &= 0.12 \pm 0.03 + (0.86 \pm 0.07)\log(R_B) \quad (G1)\\
\log(R_R) &= 0.09 \pm 0.02 + (0.78 \pm 0.02)\log(R_B) \quad (G2)\\
\log(R_R) &= 0.01 \pm 0.09 + (0.99 \pm 0.16)\log(R_B) \quad (G3)\\
\log(R_R) &= 0.06 \pm 0.01 + (0.86 \pm 0.05)\log(R_B) \quad (G4)\\
\log(R_R) &= 0.94 \pm 1.65 + (1.82 \pm 1.71)\log(R_B) \quad (G5)
\end{aligned} \tag{1}$$

with corresponding 1RMS scatters about 0.269, 0.276, 0.266, 0.328, 0.201, and 0.436, respectively. It is clear that except the objects in the G5 group, the determined best fitting results and the determined Spearman Rank correlation coefficients can be applied to confirm the robust dependence of R_R on R_B. For the dependence of R_R on R_B in the galaxies in the G5 group, although its scatter being about two times larger than those of the dependencies of the objects in the other groups and the determined slope 1.82 being not apparently larger than its corresponding uncertainty 1.71, the Spearman Rank correlation about 0.48 can be accepted to support the dependence of R_R on R_B in the objects in the G5 group. In one word, the dependence of R_R on R_B is common in the DPN galaxies collected from Ge et al. (2012). However the linear dependence can not be expected by the DGSs.

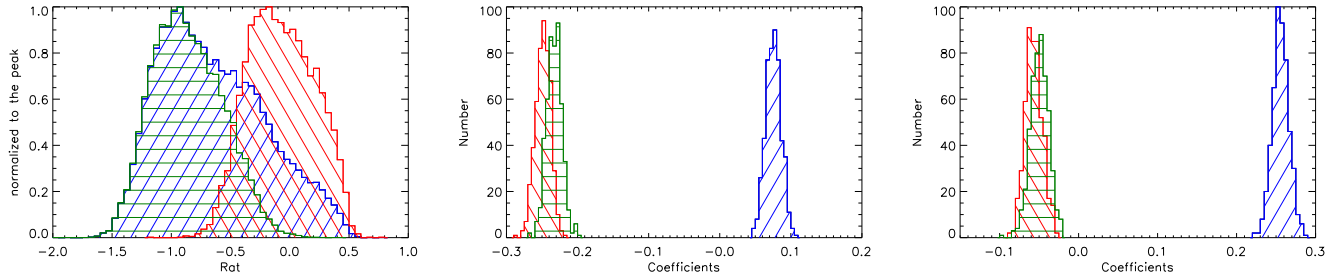

Fig. 3. Left panel shows the distributions of flux ratio of [O III]λ5007Å to narrow Hα for the AGNs (histogram filled with red lines), the HII galaxies (histogram filled with dark green lines) and all the narrow emission line galaxies (histogram filled with blue lines). Middle panel and right panel show the determined distributions of the Spearman Rank correlation coefficient, after accepted the uniform distributions (with 1 as the mean value and [0.1, 10] as the minimum and maximum values) and the Gaussian distributions (with 1 as the mean value and 0.5 as the second moment) for the peak intensity ratios.

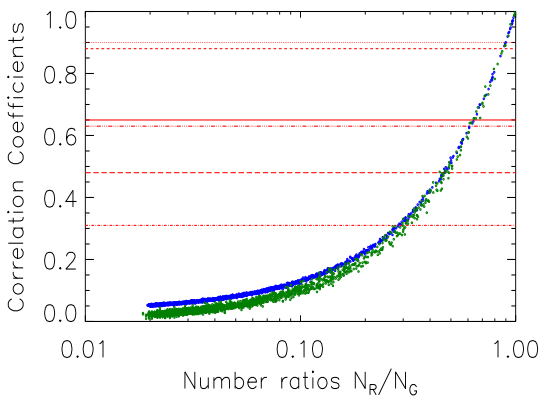

Fig. 4. On the dependence of Spearman Rank Correlation coefficient on the number ratio of N_R/N_G. Symbols in blue and in dark green show the results through all the galaxy pairs, and through the randomly collected 1618 galaxy pairs. Horizontal red solid line marks coefficient to be 0.65 for all the DPN galaxies, and horizontal red dashed lines from top to bottom show the coefficients to be 0.90, 0.88, 0.63, 0.48, 0.31 for the galaxies in the group of G1, G2, G4, G3, G5, respectively.

Before proceeding further, it is necessary to check whether there was flux connection between narrow emission lines in two nearby galaxies. In SDSS DR16 (Sloan Digital Sky Survey, Data Release 16) (Ahumada et al. 2020)), there are 77982 narrow emission line galaxies collected with redshift smaller than 0.35, and with the measured emission line fluxes at least 5 times larger than their uncertainties in the [O III]λ5007Å and in narrow Hα, and with the median spectral signal-to-noise lager than 10, and with the SDSS pipeline provided subclasses as 'AGN' or 'STARFORMING' OR 'STARBURST', and with the flux ratio of narrow Hα to narrow Hβ smaller than 6 (to ignore effects of dust obscurations). Then, among the collected 77982 narrow emission line galaxies, there are about 13000 Type-2 AGNs. Among the 13000 Type-2 AGNs, there are 669 couples of AGNs (AGN pairs) with redshift difference smaller than 0.001 and with the position distance smaller than 30arcmins. Here, if there were more than one AGN near to the target AGN within position distance smaller than 30arcmins, the one with the smallest position distance is accepted as the companion AGN to the target AGN. Then, the left panel of Fig. 2 shows the flux correlations in [O III]λ5007Å and in narrow Hα in the 669 AGN pairs, leading to the corresponding Spearman rank correlation coefficients about -0.01 (P_{null} ~ 78%) and 0.06 (P_{null} ~ 13%) for the correlations on fluxes of [O III]λ5007Å and on fluxes of narrow Hα, respectively. The right panel of Fig. 2 shows the dependence of the flux ratios of [O III]λ5007Å and of narrow Hα on the position distances in the 669 AGN pairs, leading to the corresponding Spearman rank correlation coefficients about 0.03 (P_{null} ~ 40%) and -0.002 (P_{null} ~ 97%) for the correlations on fluxes of [O III]λ5007Å and on fluxes of narrow Hα, respectively. Therefore, through the collected 669 AGN pairs, there are no narrow emission line flux correlations, nor dependence of narrow emission line flux ratios on position distances.

Meanwhile, among the 77982 narrow emission line galaxies in SDSS DR16, based on the same criteria on redshift difference smaller than 0.001 and position distance smaller than 30arcmins, there are about 3299 couples of a type-2 AGN plus a HII galaxy, and 11442 couples of HII galaxies. And the corresponding Spearman Rank correlation coefficients are not larger than 0.1 for the narrow emission line flux correlations nor for the dependencies of narrow emission line flux ratios on position distances. Moreover, criterion on smaller position distance smaller than 20arcmins (10arcmins) have also been applied, leading to smaller number of couples of narrow emission line galaxies, but leading to the similar conclusions that the corresponding Spearman Rank correlation coefficients are not larger than 0.1. Here, besides the results shown in Fig. 2 for the couples of Type-2 AGNs, there are no plots for correlations and dependencies for the other kinds of couples of narrow emission line galaxies.

Furthermore, as known, in order to detect apparent double-peaked features in narrow emission lines, the peak intensities of each DPNEL should be not very different. Therefore, it is necessary to check probable effects of peak intensity ratio on the results shown in Fig. 1. Assumed that the intensity ratio between 0.1 and 10 of two peaks in one DPNEL could lead to detectable double-peaked features, followed the distributions of the flux ratios Rat of [O III] to narrow Hα of the collected narrow emission line galaxies shown in the left panel of Fig. 3 (for AGNs, for HII galaxies, and for all the narrow emission line galaxies), total intensities (flux in arbitrary units) of [O III] and narrow Hα are artificially set to be Rat and 1. Then, random values R_3 and R_α are collected from uniform distributions (with 1 as the mean value and [0.1, 10] as the minimum and maximum values) for the intensity ratio of the red-shifted component to the blue-shifted component in the [O III] and in the narrow Hα, leading the simulated fluxes of red-shifted and blue-shifted components in [O III] and narrow Hα to be $Rat \times \frac{R_3}{1+R_3}$, $Rat \times \frac{1}{1+R_3}$, $1 \times \frac{R_\alpha}{1+R_\alpha}$ and $1 \times \frac{1}{1+R_\alpha}$. Then, the corresponding Spearman Rank correlation

coefficients can be determined between the simulated R_R and R_B. Repeating the procedure above 500times, the distributions of the coefficients are shown in the middle panel of Fig. 3. Meanwhile, if random values of R_3 and R_α are not from uniform distributions but from Gaussian distributions (with 0 as the mean value and 0.5 as the second moment in logarithmic space), the corresponding distributions of correlation coefficients are shown in the right panel of Fig. 3. It is clear that the peak intensity ratios can lead to simulated Spearman Rank correlation coefficients not larger than 0.3. Therefore, the shown results in Fig. 1 are not due to narrow range of peak intensity ratios.

Once we reasonably accept the robust conclusion that there are no correlations between narrow emission line fluxes nor dependencies of narrow emission line flux ratios on position distances in couples of narrow emission line galaxies, the DGS is not the preferred scenario to explain the results in Fig. 1. However, it will be expected that the red-shifted components and the blue-shifted components in DPNELs should have similar physical dynamical environments. Therefore, the results in Fig. 1 can be applied to roughly determine the proportion of DPN galaxies have their DPNELs are not related to DGSs.

Based on all the N_G (=669+3299+11442) couples of narrow line galaxies in SDSS DR16, N_R ($\leq N_G$) non repeating couples are randomly collected. For each selected couple, the fluxes in narrow emission lines are re-set to be equal values. Then, the corresponding Spearman rank correlation coefficient can be estimated through the newly set emission line fluxes in narrow emission lines in the N_G couples. Repeating the procedure above about 2000 times with random values of N_R, Fig. 4 shows the determined dependence of Spearman Rank correlation on the number ratio of N_R to N_G. In order to find the strong linear dependency with correlation coefficient about 0.65 for all the DPN galaxies, at least 65.5% of the dDPN galaxies have their DPNELs not related to the proposed DGSs. Moreover, different N_G = 1618 (the number of the DPN galaxies in Ge et al. 2012) has been also applied, leading to the similar results, indicating few effects of different N_G on the results shown in Fig. 4. Meanwhile, if individually considering the DPN galaxies in the G1, G2, G4, G3 and G5 groups, the corresponding number ratios are about 91.5%, 88.3%, 62.5%, 47.8% and 30.1%, respectively.

Before ending the section, three additional points are noted. First, there are different Spearman Rank correlation coefficients for the DPN galaxies in the 5 groups, however, we have no clear points on the physical origin for the different coefficients and then for the very different expected number ratios of N_R to N_G. Probably, physical dynamical environments have more apparent effects on the DPNELs in AGN related NLRs than on the DPNELs in HII related NLRs? However, the different Spearman Rank correlation coefficients and the corresponding different number ratios of N_R to N_G could probably indicate larger effects of intrinsic AGN variability on the detected DPNELs. Second, the results shown in Fig. 2 are only through the couples of nearby galaxies within 30arcmins (to 10arcmins), probably, when the merger process leading to the two NLRs close enough, probably some unknown physical mechanisms could lead to intrinsic connections between the two NLRs properties in the two galaxies undergoing the merge process. Third, based on a defined parameter R_{ps} as ratio of peak separation to the sum of the line width of the two components in each DPNEL, we have checked whether more apparent DPNELs with larger R_{ps} can lead to different results. Then, in each group, about half of the galaxies are collected by R_{ps} larger than the mean value of R_{ps}, and shown as open red circles in Fig. 1. The corresponding Spearman Rank correlation coefficients between R_R and R_B are about 0.84 ($P_{null} \sim 1.5 \times 10^{-6}$), 0.87 ($P_{null} < 10^{-21}$), 0.40 ($P_{null} \sim 2.7 \times 10^{-5}$), 0.70 ($P_{null} < 10^{-21}$) and 0.44 ($P_{null} \sim 8.9 \times 10^{-3}$) for about half of the objects with larger R_{ps} in the group of G1, G2, G3, G4, G5, respectively, similar as the results for all the galaxies in each group. Therefore, there are few effects of R_{ps} on our discussed results. On studying an independent large sample of DPN galaxies in the near future could provide further clues on understanding the discussed results.

3. Conclusions

- Through the large sample of DPNELs in SDSS, strong linear correlations can be found between R_R and R_B.
- Through the collected galaxy pairs with redshift difference smaller than 0.01 and position distance smaller than 30arcmins, there are no flux connections between narrow emission lines in the different kinds of galaxy pairs.
- Considering narrow range of peak intensity ratios for detecting DPNELs, the estimated correlation coefficients are smaller than the coefficients for the DPNELs in SDSS.
- The strong linear correlations between R_R and R_B are robust enough, strongly indicating that the commonly proposed dual galaxy system is not the preferred scenario to explain the reported DPNELs.
- Through simple simulating results on real flux ratio distributions of [O III] to narrow Hα, more than 65.5% of the DPNELs are not related to DGSs.
- Considering the DPN galaxies in G1, G2, G4, G3 and G5 groups, more than 91.5%, 88.3%, 62.5%, 47.8% and 30.1% of the DPNELs are not related to DGSs, respectively.

Acknowledgements. Zhang gratefully acknowledges the anonymous referee for giving us constructive comments and suggestions to greatly improve the paper. Zhang gratefully thanks the kind financial support from GuangXi University and the kind grant support from NSFC-12173020 and NSFC-12373014 and the Guangxi Talent Programme (Highland of Innovation Talents). This manuscript has made use of the data from the SDSS projects. The SDSS-III web site is http://www.sdss3.org/. SDSS-III is managed by the Astrophysical Research Consortium for the Participating Institutions of the SDSS-III Collaboration.

References

Ahumada, R.; Allende Prieto, C.; Almeida, A.; et al., 2020, ApJS, 249, 3
Attard, K.; Gualandris, A.; Read, J. I.; Dehnen, W., 2024, MNRAS, 529, 2150
Baldwin, J. A.; Phillips, M. M.; Terlevich, R. 1981, PASP, 93, 5
Cappellari, M.; Scott, N.; Alatalo, K.; et al., 2013, MNRAS, 432, 1709
Cole, S.; Lacey, C. G.; Baugh, C. M.; Frenk, C. S., 2000, MNRAS, 319, 168
Comerford, J.M.; Gerke, B.F.; Newman, J.A.; et al, 2009, ApJ, 698, 956
Comerford, J.M.; Nevin, R.; Stemo, A., et al, 2018, ApJ, 867, 66
De Lucia, G.; Blaizot, J., 2007, MNRAS, 375, 2
Fu, H.; Yan, L.; Myers, A.D., et al., 2012, ApJ, 745, 67
Ge, J. Q., Hu, C., Wang, J. M., et al., 2012, ApJS, 201, 31
Kauffmann, G.; Heckman, T. M.; Tremonti, C., et al., 2003, MNRAS, 346, 1055
Kewley, L. J.; Dopita, M. A.; Sutherland, R. S.; Heisler, C. A.; Trevena, J., 2001, ApJ, 556, 121
Kewley, L. J.; Groves, B.; Kauffmann, G.; Heckman, T., 2006, MNRAS, 372, 961
Kewley, L. J.; Nicholls, D. C.; Sutherland, R. S., 2019, ARA&A, 57, 511
Mahdi R.; Mohammad A., 2017, J. Statistical Computation and Simulation, 87, 1130
Maschmann, D., Melchior, A.L., Mamon, G. A., et al., 2020, A&A, 641, 171
Merritt, D., 2006, ApJ, 648, 976
Nevin, R.; Comerford, J.; Muller-Sanchez, F.,et al, 2016, ApJ, 832, 67
Rubinur, K.; Das, M.; Kharb, P., 2019, MNRAS, 484, 4933
Satyapal, S.; Ellison, S. L.; McAlpine, W.; Hickox, R. C.; Patton, D. R.; Mendel, J. T., 2014, MNRAS, 441, 1297
Shen, Y.; Liu, X.; Greene, J.E., et al, 2011a, ApJ, 735, 48
Silk, J.; Rees, M. J. 1998, A&A, 331, L1
Smith, K.L.; Shields, G.A.; Bonning, E. W., et al, 2010, ApJ, 716, 866
Volonteri, M.; Haardt, F.; Madau, P., 2003, ApJ, 582, 559
Wang, J. M.; Chen, Y. M.; Hu, C., et al, 2009, ApJ, 705, 76
Wang, M. X.; Luo, A. L.; Song, Y. H., et al, 2019, MNRAS, 482, 1889
Yoon, Y.; Park, C.; Chung, H.; Lane, R. R., 2022, ApJ, 925, 168
Zoldan, A.; De Lucia, G.; Xie, L.; Fontanot, F.; Hirschmann, M., 2019, MNRAS, 487, 5649
Zhang, X. G.; Feng, Y. Q.; Chen, H.; Yuan, Q. R., 2020, ApJ, 905, 97
Zheng, Q.; Ma, Y.; Zhang, X. G.; Yuan, Q.; Bian, W., 2025, ApJS, 277, 49
Zhou, H. Y.; Wang, T. G.; Zhang, X. G., et al, 2004, ApJ, 604, 33